Neutron scattering on magnetic thin films: Pushing the limits (invited)

A. Schreyer,[a] T. Schmitte, R. Siebrecht, P. Bödeker, and H. Zabel
Institut für Experimentalphysik/Festkörperphysik, Ruhr-Universität Bochum, D-44780 Bochum, Germany

S. H. Lee, R. W. Erwin, and C. F. Majkrzak
National Institute of Standards and Technology, Gaithersburg, Maryland 20899

J. Kwo and M. Hong
Lucent Technologies, Bell Laboratories, Murray Hill, New Jersey 07974

Neutron scattering has been the scattering technique of choice for the analysis of magnetic structures and their dynamics for many decades. The advent of magnetic thin film systems has posed new challenges since such samples have inherently small scattering volumes. By way of examples, recent progress in the application of neutron scattering for the study of both magnetic structure and dynamics in magnetic thin film systems will be presented. First, a combined high angle neutron scattering and polarized neutron reflectivity investigation of the magnetic order of Cr and its influence on the exchange coupling between the Fe layers in Fe/Cr superlattices is discussed. It is shown that in the whole thickness range up to 3000 Å, the magnetic structure is governed by frustration effects at the Fe/Cr interfaces. Second, it is demonstrated that it is now possible to investigate the dynamic properties of magnetic thin films with neutron scattering. Unlike, e.g., Brillouin light scattering, inelastic neutron scattering provides access to large portions of the Brillouin zone. First results on spin wave excitations in a Dy/Y superlattice are presented. © *2000 American Institute of Physics.* [S0021-8979(00)92908-6]

I. INTRODUCTION

Neutron scattering has been the scattering technique of choice for the analysis of magnetic structures and their dynamics for many decades. Due to advances in preparation techniques in the last decade, research in magnetism has moved more and more towards the investigation of layered magnetic thin film structures. A wealth of effects has been discovered which modify the magnetic structure, the dynamics, and the transport properties in magnetic thin films compared to bulk.[1] This development has posed new challenges for neutron scattering since such samples have inherently small scattering volumes. In this article, we will outline a few examples of recent progress which has been made in the application of neutron scattering techniques for research in magnetic thin film structures.

Polarized neutron reflectometry (PNR) clearly is a very important technique in the field. However, since it is covered by Gian Felcher in this volume, we will focus on complementary recent developments. PNR is performed at small scattering vectors $Q=4\pi/\lambda \sin\theta$ up to $0.4\,\text{Å}^{-1}$. Here, λ is the neutron wavelength and θ is the scattering angle. This scattering vector range is well suited to investigate magnetization profiles of thin film structures which may exhibit periodicities on the order of tens of Å. However, PNR does not provide information on the magnetic order on the atomic scale. To obtain such information, scattering vectors on the order of a few Å^{-1} are required, i.e., classical high angle scattering techniques must be used. Recently, instruments such as ADAM[2] at the Institut Laue Langevin in Grenoble/France have been built, which can provide access to small *and* high Q in one experiment.

The use of strong dynamical scattering effects, like the strong reflectivity increase towards total reflectivity at very small Q (Fresnel reflectivity), can effectively increase the scattering signal in PNR. At high scattering angles, no such effects occur. The scattering is simply proportional to the number of scattering atoms. Thus, if information on magnetic order on atomic length scales is required, even more attention must be given to the use of samples with sufficient scattering volume.

II. ELASTIC SCATTERING

The magnetic structure of Cr in thin films and superlattices is such a problem. Cr exhibits a complicated spin density wave magnetic structure in bulk.[3] Historically, epitaxial Fe/Cr structures have played a key role in thin film magnetism. The oscillatory exchange coupling, the giant magnetoresistance effect and the noncollinear coupling have been discovered in Fe/Cr.[4] Fe/Cr differs from most other systems, which also show these properties, due to the inherent Cr antiferromagnetism. Thus, the question is how any magnetic order of the Cr correlates with the exchange coupling between the Fe layers. In the following, we review a recent combined high angle neutron scattering and PNR investigation of the magnetic order of Cr and its influence on the exchange coupling between the Fe layers. It will be shown that the details of the magnetic Cr structure and the exchange coupling are governed by frustration at the Fe/Cr interfaces over the whole thickness range investigated.

Since Cr has only a small magnetic moment of about $0.55\mu_B$, the magnetic neutron scattering cross section is

[a]Electronic mail: andreas.schreyer@uni-bochum.de

quite weak. This requires special efforts to maximize the scattering volume for high angle neutron experiments. We have grown a series of Fe/Cr samples with a fixed Fe thickness of 20 Å and the Cr thickness varying between 10 and 3000 Å by molecular-beam epitaxy (MBE) methods on a Nb buffer using large 2 in.×2 in. sapphire substrates.[6–8] To obtain sufficient scattering volume, Fe/Cr superlattice samples with up to 250 bilayer repeats were used for the smallest Cr thicknesses t_{Cr}. For $t_{Cr} > 1000$ Å, a single Cr film between the Fe layers was sufficient.

Bulk Cr is antiferromagnetic, i.e., the moments at the center of the Cr bcc structure are aligned opposite to those on the corners. This simple structure is called a commensurate spin density wave (CSDW). Superimposed on this structure is a sinusoidal modulation of the magnitude of the antiferromagnetically aligned Cr moments μ with a period Λ_{ISDW}. Since Λ_{ISDW} is incommensurate with the Cr lattice this magnetic structure is classified as an incommensurate spin density wave (ISDW). Λ_{ISDW} is about 21 lattice constants at $T=0$ and increases with temperature.[3] The incommensurability is ascribed to a nesting vector along the {100} directions of the Cr Fermi surface. The wave vector **q** defines the direction of propagation of the ISDW. At lowest temperatures a longitudinal ISDW (LSDW) forms, i.e., $\boldsymbol{\mu}$ is parallel to **q**. Above the spin-flip transition temperature, $T_{SF}=123$ K, $\boldsymbol{\mu}$ is perpendicular to **q**, forming a transverse ISDW (TSDW). Above $T_N=311$ K bulk Cr is paramagnetic.

The incommensurate modulation of the antiferromagnetic (AF) spin structure by the ISDW causes *two* satellite peaks to occur around the {1,0,0} positions,[3] e.g., at $(0,0,1\pm\delta)$, $(1\pm\delta,0,0)$, and $(0,1\pm\delta,0)$ which can be investigated by neutron scattering. Here, $\delta=1-|\mathbf{q}|$ with $|\mathbf{q}|$ in reciprocal lattice units, $\delta=a/\Lambda_{ISDW}$, and the Cr lattice constant a. In the first case, the position of the satellites indicates **q** being oriented along the out of the film plane L axis, the two latter cases occur for either direction of in-plane propagation along *H* or *K*. In addition, the polarization of the ISDW (i.e., TSDW or LSDW) can be obtained by making use of the selection rules for magnetic neutron scattering. It requires a component of the magnetization vector $\boldsymbol{\mu}$ to be perpendicular to the scattering vector $|\mathbf{Q}|$. Thus, a LSDW propagating along L, i.e., out-of-plane, will generate no intensity at $(0,0,1\pm\delta)$. However, satellites will occur at $(1,0,0\pm\delta)$. On the other hand, a TSDW propagating along *L*, will produce peaks at $(0,0,1\pm\delta)$, whereas no intensity will occur at $(1,0,0\pm\delta)$. A CSDW phase, on the other hand, will yield a *single* peak of purely magnetic origin exactly at the Cr{001} positions due to the commensurability with the Cr lattice. Thus, with neutron scattering we can uniquely distinguish CSDW and ISDW magnetic order as well as ISDW propagation and polarization. For a more detailed discussion, see, e.g., Ref. 8.

A. Thin Cr films

First, we briefly review the results for small t_{Cr}, where the Cr mediates an exchange coupling between the Fe layers.[4] For $t_{Cr}=42$ Å, Cr is found to exhibit CSDW order. Superimposed on this magnetic order we find a spiral modulation which is induced by lateral Cr thickness variations.[6]

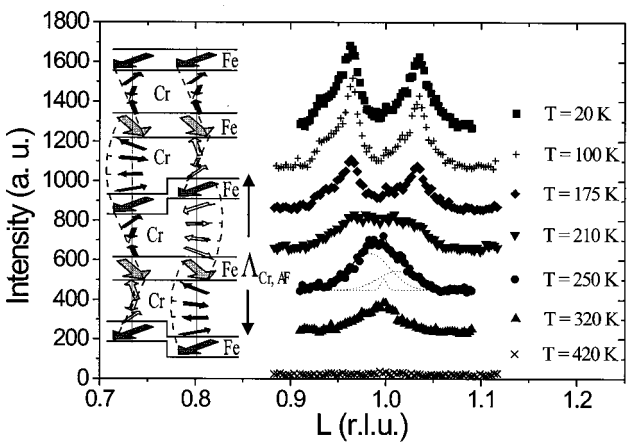

FIG. 1. Neutron scans along *L* through (001) as a function of temperature *T* for a sample of composition $[Cr_{80}/Fe_{19}]_{133}$. The scattering vector *Q* is plotted in reciprocal lattice units (r.l.u.) and denoted according to the corresponding axis of the reciprocal lattice. For the 250 K data, the distance of the two fitted broad peaks from the central peak corresponds to $\Lambda_{Cr,AF}=2\Lambda_{SL}=\Lambda_{Fe,NC}$. The inset depicts the model obtained from the fitted data.

This complicated magnetic structure mediates a noncollinear coupling between the Fe layers, as is shown by PNR. A schematic picture is provided in the inset of Fig. 1. A lateral Cr thickness variation on average leads to a lateral coexistence of even and uneven number of Cr layers. The coupling of the Cr to the Fe is assumed to be the same at all top and bottom Fe/Cr interfaces, respectively. Then, partial spirals of opposing sense of rotation are the topologically simplest way to accommodate the Cr between the noncollinear Fe layers. Since the Cr tends to be a collinear antiferromagnet, each of the spirals applies a torque. However, due to the opposing sense of rotation of the laterally coexisting spirals, the torque is frustrated. Neither can an even number of Cr layers rotate the Fe layers antiparallel, nor can an uneven number of Cr layers rotate the Fe layers parallel. Instead, the Fe layers choose a compromise. They align noncollinearly at roughly 90°. This spiral magnetic structure had originally been proposed by Slonczewski within his proximity magnetism model.[9] Above the Néel temperature of this magnetic Cr order, the frustration vanishes. Consequently, the noncollinear order also vanishes.[6]

It is important to point out that so far we have considered a case where $t_{Cr} \ll \Lambda_{ISDW}$. The observation of a commensurate SDW instead of an ISDW can be attributed to the fact that the Cr is too thin to support an ISDW. This will obviously change at larger Cr thicknesses. In Fig. 1, neutron (00L) scans through (001) are shown for a $[Cr_{80}/Fe_{19}]_{133}$ sample as a function of temperature. Unlike at $t_{Cr}=42$ Å, [6] the form of the spectra changes drastically as a function of temperature. For $T=20$ K, a double peak structure around (001) is found, as is typical for a TSDW propagating along the film growth direction (L). In the present case, t_{Cr} is on the order of Λ_{ISDW}, i.e., one ISDW period fits into each Cr layer along the growth axis. Thus, it is plausible that an ISDW can form. The ISDW period of $\Lambda_{ISDW}=79$ Å determined from the peak positions at $(0,0,1\pm\delta)$ is somewhat enhanced compared to bulk values.[8] Also, weak second-

order harmonics at $(0,0,1\pm 2\delta)$ are observed, which do not occur in bulk[3] indicating a more square waveform of the ISDW than in bulk. It is tempting to attribute this effect to the finite Cr thickness. The squaring can actually be viewed as a precursor of the transition from ISDW to CSDW which occurs as we reduce t_{Cr}.

With increasing temperature, a dramatic change of the spectrum is observed in Fig. 1: The line shape changes from a predominantly double peak to a broad peak at (001) at $T=250\,K$ which is very much reminiscent of the data for $t_{Cr}=42\,Å$.[6] As is shown in the figure, the data fits well to the same model, as the $t_{Cr}=42\,Å$ data, i.e., to a sharp central Gaussian and two broad superlattice satellite peaks. Their distance to the central peak corresponds to twice the superlattice periodicity Λ_{SL} and is equal to the periodicity $\Lambda_{Fe,NC}$ of the noncollinearly coupled Fe layers, i.e., $\Lambda_{Cr,AF}=2\Lambda_{SL}=\Lambda_{Fe,NC}$. Inspection of the figure in the inset shows that this relation holds for the depicted model structure. As detailed in Ref. 6, the disorder along the growth direction of the model structure induces the observed broadening of the satellite peaks. Structure factor calculations and polarized neutron measurements confirm that the frustrated spiral structure shown in the inset causes the observed scattering. Thus, we find a transition from an ISDW at low temperatures to the frustrated spiral CSDW at elevated temperatures.[10] This transition can be explained by the increase of the ISDW period with temperature, as it occurs in bulk: For a given t_{Cr}, a single ISDW period can form below a certain temperature. If the temperature rises above this value, the LRO changes to a CSDW.

An obvious question at this point is if the exchange coupling between the Fe layers changes with the transition from the ISDW to the frustrated CSDW Cr structure. In Fig. 2, temperature-dependent magneto-optical Kerr effect (MOKE) data is shown. At low temperatures, the hysteresis loop is nearly square, indicating very weak or no coupling. Above a broad transition region,[10] a hysteresis curve typical of noncollinear coupling is found. PNR measurements have confirmed these results. Thus, we observe a transition from essentially no coupling between the Fe layers to NC coupling, as the Cr structure transforms from ISDW to the frustrated spiral CSDW for a sample with $t_{Cr}=80\,Å$.

The detailed functional form of the region of existence of the ISDW phase as a function of t_{Cr} and temperature has been mapped out by Fullerton *et al.*[11,12] using MOKE hysteresis loops, resistance measurements, and neutron scattering. The phase boundary which they obtain is fully consistent with our data. As in our case, they also find that the coupling between the Fe layers vanishes, as soon as the ISDW occurs. However, they do not observe the occurrence of the strong CSDW signal as the ISDW vanishes with increasing temperature. This is most probably due to a difference in the structure of the Fe/Cr interfaces. It has been shown by Slonczewski that the average distance between steps in the Fe/Cr interface, which effectively change the Cr thickness, must be on the order of 100 Å, consistent with our data.[6] Otherwise, the specific frustrated structure observed here does not form. Since the samples of Fullerton *et al.* had been prepared by a different technique (sputtering) on a different kind of substrate than in the present case, it is to be expected that in their case the distance between the steps is much smaller. Any antiferromagnetic order in the Cr layers would still be highly frustrated. However, the correlation length of this frustrated structure could be so small, that it might not yield sufficiently strong peaks which are observable with neutron scattering. Nevertheless, such a frustrated structure could still mediate the observed noncollinear coupling between Fe layers.

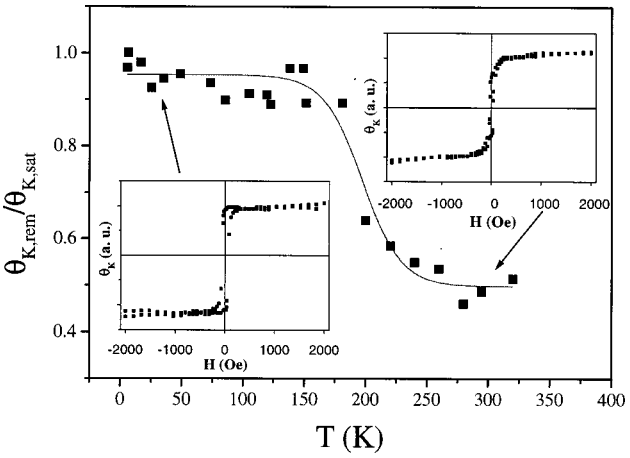

FIG. 2. Kerr rotation in remanence normalized by Kerr rotation in saturation as a function of temperature for the same sample as in Fig. 1. In the insets, complete hysteresis loops are shown for the temperatures indicated by the arrows. The data indicate a transition from uncoupled behavior to NC coupling with increasing temperature.

The absence of coupling between the Fe layers in the ISDW phase at low temperatures can be understood in the following way. Apparently, the ISDW minimizes the frustration of the Fe/Cr interlayer coupling, which is induced by imperfect Fe/Cr interfaces, by moving its nodes to the Fe/Cr interfaces.[12] The small magnetic Cr moments at the ISDW nodes then can effectively decouple the ISDW Cr from the ferromagnetic Fe, strongly reducing any interlayer exchange coupling.

Shi and Fishman have studied the magnetic structure of Cr in Fe/Cr theoretically.[13] For ideal Fe/Cr interfaces, they predicted the observed ISDW to CSDW transition as a function of temperature and Cr thickness. In a more recent paper,[14] Fishman considered more realistic interfaces with steps. He finds *helical* SDWs (HSDW) corresponding to the spiral magnetic structure proposed by Slonczewski, confirming the frustration effect as the cause of the noncollinear coupling between the Fe layers. Interestingly, he predicts for $t_{Cr}=80\,Å$ that the HSDW performs a 270° twist instead of only a 90° rotation as shown in the inset of Fig. 1. So far our data do not confirm this effect.

B. Proximity effect

Most recently, we have extended our study to $t_{Cr}<42\,Å$.[15] We obtain strong evidence that the Néel temperature T_N of the frustrated CSDW increases as we reduce t_{Cr}. This behavior is contrary to expectation, since scaling theory would suggest a reduction of T_N with t_{Cr}.[16] We attribute this to a proximity effect between the Fe and the Cr. The Fe

layers have a much higher ordering temperature T_C in bulk than Cr and remain ferromagnetic at $T_{Fe}=20$ Å, as is seen in our experiments. In this case, Fe is expected to polarize the Cr atoms near the Fe/Cr interface and to induce magnetic order, which would not exist otherwise.[9] In this scenario, it can be expected that the Cr ordering temperature will increase as we reduce t_{Cr}, since the influence of the Fe will increase strongly toward the Fe/Cr interfaces. This proximity effect was such a basic assumption in Slonczewski's proximity magnetism model[9] that he named the model accordingly. Only this assumption enabled him to postulate the existence of a specific magnetic structure as the origin of NC coupling in layered systems consisting of FM and AF materials. Our observation of magnetic order and an increasing T_N with reduced t_{Cr} strongly supports the existence of a proximity effect in Fe/Cr layered systems experimentally.

Another way to test this proximity effect is to vary the ordering temperature T_C of the FM material, and to study the effect on the ordering temperature T_N of the AF material. One would then expect that T_N is reduced with T_C. We have performed such a study using the system $Fe_{1-x}Cr_x/Cr$. For increasing x between 0 and 0.8, the T_C of bulk $Fe_{1-x}Cr_x$ drops from the value of pure Fe to nearly zero. Above $x=0.8$, the system enters a spin glass state.[17] Since $Fe_{1-x}Cr_x$, Fe and Cr have the same lattice structure and nearly equal lattice constants $Fe_{1-x}Cr_x/Cr$ layered structures can be grown in similar quality as Fe/Cr, making the system an ideal candidate for such a study of the proximity effect. The experiments were performed as a function of x on a series of samples with $t_{Cr}\approx 30$ Å and $t_{FeCr}\approx 30$ Å. $T_C(Fe_{1-x}Cr_x)$ was determined via measurements of the magnetization using PNR and MOKE,[18] whereas $T_N(Cr)$ was measured using high angle neutron scattering on the AF Cr peaks. We find that $T_N(Cr)$ drops with $T_C(Fe_{1-x}Cr_x)$ as would be expected for a proximity effect. The weaker the ferromagnetism of the proximity $Fe_{1-x}Cr_x$ layer is, the less it can polarize the Cr, reducing its $T_N(Cr)$. The data and more details of the measurements on the $Fe_{1-x}Cr_x/Cr$ system will be reported elsewhere.[19,20]

C. Thick Cr films

Last but not least, we briefly review our results for very large t_{Cr}. As is shown above, we observe a TSDW for $t_{Cr}=80$ Å. Neutron scattering data show that with increasing t_{Cr}, the TSDW reorients itself between $250\text{ Å}<t_{Cr}<2000$ Å from propagating along the film growth axis to in-plane propagation with the Cr moments oriented out of the film plane.[7,8] This reorientation transition again is caused by steps at the Fe/Cr interface. These steps frustrate the system since the ferromagnetic coupling within the Fe, the antiferromagnetic coupling within the Cr and the antiferromagnetic coupling between the Fe and the Cr at the Fe/Cr interface[21] cannot be satisfied at the same time.

Calculations within a classical Heisenberg model reproduce the observed reorientation transition as soon as steps in the Fe/Cr interface are assumed.[7] For small t_{Cr}, the frustration can be accommodated by forming domain walls connecting the steps at opposing Fe/Cr interfaces *through* the Cr layers. With increasing t_{Cr}, however, the domain wall energy of such domains increases so much that the system chooses a different way to accommodate the frustration. Instead it effectively breaks the antiferromagnetic coupling between Cr and Fe at the Fe/Cr interface and reorients the Cr moments perpendicular to the Fe moments.

D. Grazing incidence diffraction

Interestingly, during the reorientation transition with increasing t_{Cr} an additional CSDW phase occurs with the moments parallel to the TSDW, i.e., out of the film plane. To establish, if the CSDW and TSDW phases coexist laterally in the film plane or stacked in layers, grazing incidence diffraction (GID) was performed with neutrons on the EVA diffractometer at the Institut Laue Langevin in Grenoble/France.[22] By varying the incident angle in the regime of total external reflection, the penetration depth of the neutrons into the sample can be tuned.[23] Thus, GID can distinguish if one of the two phases alone exists near the sample surface, indicating a layering of the two phases. The measurements were carried out on a 3000 Å thick Cr film with 20 Å Fe on top at $T=50$ K with the in-plane scattering vector aligned either with the commensurate (100) peak or with an incommensurate (0.953 0 0) ISDW reflection. An ISDW peak originating from near the sample surface was found, whereas an equivalent scan at the CSDW (100) position yielded no such peak.[22] Therefore, we can conclude that near the Fe/Cr interface the ISDW prevails. The commensurate reflections observed with conventional high angle neutron scattering must come from deep within the film. Consequently the occurrence of the commensurate phase in this system appears not to be induced by the top Fe/Cr interface, but rather by the bottom Cr/Nb interface.

As is discussed in detail in Ref. 8, the large lattice misfit between Cr and Nb at the Cr/Nb interface induce strain and a very small crystalline coherence in the film plane. Apparently, this small in-plane coherence prevents the formation of an in-plane TSDW similar to the suppression of the ISDW at small t_{Cr}. Instead, a CSDW forms. Further away from the Cr/Nb interface the crystalline quality improves allowing the formation of a TSDW. For out-of-plane propagation of the TSDW for $45\text{ Å}<t_{Cr}<250$ Å, on the other hand, the out-of-plane crystalline coherence length is found to be much larger than along the in-plane direction. Thus, no concomitant CSDW forms. This argument also holds for those samples where the Cr does not directly touch the Nb due to an intervening Fe layer. Since the Fe always was only 20 Å thick, it cannot relieve the strain induced by the Nb.

E. Conclusions

In conclusion, we have discussed results obtained on the magnetic structure of Cr by neutron scattering methods. To be able to perform neutron experiments, it was important to maximize the scattering volume by using large substrates and, for small t_{Cr}, many Fe/Cr bilayer repeats. Thus, the preparation of samples specially designed for neutron scattering is important if one wants to push the limits of neutron scattering in thin film research. This has enabled us to ob-

serve a novel frustrated spiral CSDW order in Cr films, which are only 42 Å thick. This magnetic order causes the noncollinear coupling between the Fe layers. In this regime, we also observe a proximity effect between the Fe and the Cr. As we increase t_{Cr}, the Cr layers become thick enough to support a TSDW propagating out of the film plane. At high temperatures, this TSDW transforms into the frustrated CSDW, causing noncollinear coupling between the Fe layers. As we increase t_{Cr} further, the frustration at the Fe/Cr interfaces causes a reorientation of the TSDW propagation to in-plane. A concomitant CSDW is observed, which is shown to be limited to the region near the bottom Cr/Nb interface using neutron GID. This latter technique operates at the limits of what neutrons can do. Nevertheless, if the samples are optimized accordingly, meaningful results can be extracted.

III. INELASTIC SCATTERING

So far, we have only considered elastic neutron scattering on magnetic thin films. However, inelastic neutron scattering has historically been just as important an application in condensed matter science. For neutron wavelengths in the Å range, the neutron energies happen to be well matched, e.g., to phonon and magnon excitation energies in condensed matter. However, the cross sections of this inelastic scattering are orders of magnitudes smaller, than in the elastic case. Thus, if elastic neutron scattering already poses a challenge in thin film research, inelastic neutron scattering will be even harder. However, in the following, we demonstrate that even inelastic measurements on thin film systems are possible.

Up to now, information on magnetic excitations in magnetic thin films and superlattices has come from inelastic light scattering (Brillouin scattering, BS)[24,25] and ferromagnetic resonance (FMR) experiments.[26] FMR can probe spin waves at the center of the Brillouin zone (BZ), and at magnon wave vectors q_m inversely proportional to the film thickness. With Brillouin scattering, wave vectors on the order of the wave vector of light are accessible, i.e., also close to the BZ center. Thus, it has not been possible to determine the dispersion of spin waves in magnetic thin film systems in the whole BZ.

With inelastic neutron scattering (INS), on the other hand, the dispersion of spin waves in much larger portions of the BZ is, in principle, accessible. Smaller wavelength (higher q_m) spin waves on the order of the superlattice periodicity would become accessible which can be dominated by the magnetic exchange coupling between the magnetic layers. Thus, INS would open up the possibility to study the dynamic behavior of the exchange coupling in magnetic superlattices, which was not possible so far.

Thin film samples made from rare-earth materials are the prime candidates for a study of magnetic excitations with inelastic neutron scattering, since the rare earths exhibit the largest magnetic moments of all elements, causing the largest possible cross-section for magnetic neutron scattering. Rare-earth superlattices have been studied intensely over the last decade using *elastic* neutron scattering to determine their magnetic structures.[27,28]

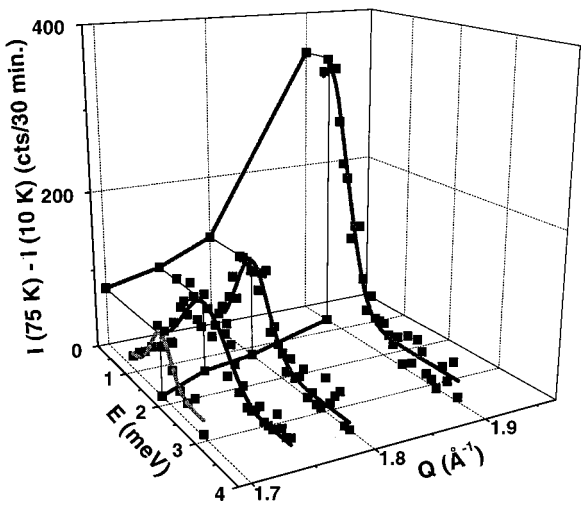

FIG. 3. Difference spectrum of inelastic neutron scattering data taken at 75 and at 10 K with Gaussian fits and the resulting dispersion curve plotted in the Q-E plane.

The *inelastic* measurements were performed on a superlattice of the layer sequence $Y_{500\,Å}[Dy_{43\,Å}/Y_{28\,Å}]_{350}/Y_{2340\,Å}/Nb_{2000\,Å}/Al_2O_3$(substrate), which was grown by MBE methods[29] along the c-axis of the hcp structure of Dy and Y. Again, the amount of Dy in the sample was maximized by growing 350 bilayers and using a rather large 1 in.$\times$0.5 in. substrate. Nevertheless, the Dy in the sample amounts to only 10 mg. Below its bulk Neél temperature of 179 K, Dy exhibits a helical phase which transforms into a ferromagnetic structure below 89 K. In Dy/Y superlattices, a coherent helical phase occurs which extends over many bilayers whereas the ferromagnetic phase is suppressed due to magnetoelastic effects.[30] The coherent helical phase is mediated by the paramagnetic Y interlayers via *RKKY* exchange coupling. Elastic neutron scattering experiments have confirmed that the present Dy/Y sample exhibits the same long-range helical order observed previously.

The neutron scattering experiments were performed at the NIST Center for Neutron Research on the cold neutron spectrometer NG-5. A focusing analyzer was used for the inelastic measurements to maximize intensity while sacrificing resolution in Q.

The inelastic measurements were performed at 75 K to create a sufficiently large spin-wave scattering cross section.[31] Equivalent scans at 10 K, where the spin-wave cross section is negligible, serve as a quasi-background. The intensity difference of these scans then is a good measure of the spin-wave cross section. Counting for about 30 min per point was necessary to obtain the data summarized in Fig. 3, where the difference between the 75 and 10 K data sets is plotted together with Gaussian fits and the projections of the peaks onto the Q-I and Q-E planes. We find a spin-wave excitation, which is well-localized in energy. The resulting dispersion curve is shown in the Q-E plane. Its extrapolation to higher Q yields an elastic peak at 1.97 Å^{-1} as its origin. This peak is caused by the helical long-range magnetic order in the superlattice. Comparison with the data of bulk Dy[32]

shows that the dispersion curve observed here is essentially consistent with the bulk curve.

These data demonstrate that it is possible to measure spin wave excitations in magnetic superlattices. A number of interesting questions can now be investigated. In a superlattice the additional superlattice periodicity should lead to a folding of the Brillouin zone.[33] Furthermore, it is expected, that the coupling between the Dy layers via the Y modifies the dispersion in a certain q_m range. Gaps could exist at the boundaries of the folded Brillouin zone. Most recent higher resolution measurements provide strong evidence for these effects. These results will be reported elsewhere.[34]

IV. CONCLUSIONS

In conclusion, we have presented not only elastic but also inelastic neutron scattering measurements on magnetic thin film samples. The latter was not possible up to now. The key is to provide samples of sufficient scattering volume. In combination with modern neutron instrumentation at high flux sources, this will provide new insights into the magnetic structure and dynamics which may not be obtainable otherwise.

ACKNOWLEDGMENTS

The authors acknowledge financial support from the Bundesministerium für Bildung und Forschung (03-ZA5BC20) and the Deutsche Forschungsgemeinschaft (SFB 166). One of the authors (A.S.) is indebted to the Alexander von Humboldt Foundation for a Feodor Lynen fellowship during which the work on the inelastic measurements was begun.

[1] See, e.g., *Ultrathin Magnetic Structures I+II*, edited by B. Heinrich and J. A. C. Bland (Springer, Berlin, 1994).
[2] A. Schreyer, R. Siebrecht, U. Englisch, U. Pietsch, and H. Zabel, Physica B **248**, 349 (1998).
[3] For a review, see, e.g., E. Fawcett, Rev. Mod. Phys. **60**, 209 (1988).
[4] For an overview and a list of references, see, for example, Ref. 5.
[5] A. Schreyer, J. F. Ankner, Th. Zeidler, H. Zabel, M. Schäfer, J. A. Wolf, P. Grünberg, and C. F. Majkrzak, Phys. Rev. B **52**, 16066 (1995).
[6] A. Schreyer, C. F. Majkrzak, Th. Zeidler, T. Schmitte, P. Bödeker, K. Theis-Bröhl, A. Abromeit, J. A. Dura, and T. Watanabe, Phys. Rev. Lett. **79**, 4914 (1997).
[7] P. Bödeker, A. Hucht, A. Schreyer, J. Borchers, F. Güthoff, and H. Zabel, Phys. Rev. Lett. **81**, 914 (1998).
[8] P. Bödeker, A. Schreyer, and H. Zabel, Phys. Rev. B **59**, 9408 (1999).
[9] J. C. Slonczewski, J. Magn. Magn. Mater. **150**, 13 (1995).
[10] According to the more complete data shown here, the transition region between the ISDW and CSDW phases extends roughly from 150 to 250 K. Thus, the transition region is somewhat smaller than shown in Fig. 1 of Ref. 6.
[11] E. E. Fullerton *et al.*, Phys. Rev. Lett. **75**, 330 (1995).
[12] E. E. Fullerton, S. D. Bader, and J. L. Robertson, Phys. Rev. Lett. **77**, 1382 (1996).
[13] Z. P. Shi and R. S. Fishman, Phys. Rev. Lett. **78**, 1351 (1997).
[14] R. S. Fishman, Phys. Rev. Lett. **81**, 4979 (1998).
[15] T. Schmitte, A. Schreyer, V. Leiner, R. Siebrecht, K. Theis-Bröhl, and H. Zabel, Europhys. Lett. **48**, 692 (1999).
[16] K. Binder, in *Phase Transitions and Critical Phenomena*, edited by C. Domb and J. L. Lebowitz (Academic, London, 1983), pp. 1–144.
[17] Landolt-Börnstein, *Zahlenwerte und Funktionen aus Naturwissenschft und Technik*, Gruppe 3: Kristall- und Festkörperphysik. N-S.; Magnetische Eigenschaften von Metallen (Springer, Berlin, 1986).
[18] R. Siebrecht, A. Schreyer, T. Schmitte, W. Schmidt, and H. Zabel, Physica B **267–268**, 207 (1999).
[19] R. Siebrecht, Ph.D. thesis, Ruhr-Universität Bochum, Germany (in preparation).
[20] R. Siebrecht, A. Schreyer, T. Schmitte, W. Schmidt, and H. Zabel (unpublished).
[21] See, e.g., F. U. Hillebrecht *et al.*, Europhys. Lett. **19**, 711 (1992).
[22] P. Bödeker, A. Schreyer, P. Sonntag, Ch. Sutter, G. Grübel, and H. Zabel, Phys. Rev. B **248**, 115 (1998).
[23] H. Dosch, *Critical Phenomena at Surfaces and Interfaces*, Springer Tracts in Modern Physics (Springer, Berlin, 1992), Vol. 126.
[24] P. Grünberg, in *Light Scattering in Solids V*, edited by M. Cardona and G. Güntherodt (Springer, Berlin, 1989).
[25] B. Hillebrands and G. Güntherodt, in Ref. 1, Vol. II, pp. 258–277.
[26] B. Heinrich, in Ref. 1, Vol II, pp. 195–257.
[27] C. F. Majkrzak *et al.*, Adv. Phys. **40**, 99 (1991).
[28] D. F. McMorrow *et al.*, Physica B **192**, 150 (1993).
[29] J. Kwo, in *Thin Film Techniques for Low Dimensional Structures*, edited by R. F. C. Farrow, S. S. S. Parkin, P. J. Dobson, N. H. Neaves, and A. S. Arrott, NATO ASI Series B, Physics V13 (Plenum, New York, 1988), p. 337; M. Hong, R. M. Fleming, J. Kwo, L. F. Schneemeyer, J. V. Waszczak, J. P. Mannaerts, C. F. Majkrzak, D. Gibbs, and J. Bohr, J. Appl. Phys. **61**, 4052, (1987).
[30] M. B. Salomon *et al.*, Phys. Rev. Lett. **56**, 259 (1986).
[31] See, e.g., G. L. Squires, *Introduction to Thermal Neutron Scattering* (Cambridge University Press, Cambridge, New York, 1978).
[32] R. M. Nicklow *et al.*, Phys. Rev. Lett. **26**, 140 (1971).
[33] See, for example, J. Sapriel and B. Djafari Rouhani, Surf. Sci. Rep. **10**, 189 (1989).
[34] A. Schreyer *et al.* (unpublished).